symmetry

MDPI

Article

Parallel Raster Scan for Euclidean Distance Transform

Juan Carlos Elizondo-Leal [1,*], José Gabriel Ramirez-Torres [2], Jose Hugo Barrón-Zambrano [1], Alan Diaz-Manríquez [1], Marco Aurelio Nuño-Maganda [3] and Vicente Paul Saldivar-Alonso [1]

1 Facultad de Ingeniería y Ciencias, Universidad Autónoma de Tamaulipas, Ciudad Victoria 87149, Mexico; hbarron@docentes.uat.edu.mx (J.H.B.-Z.); amanriquez@docentes.uat.edu.mx (A.D.-M.); vpsaldiv@docentes.uat.edu.mx (V.P.S.-A.)

2 Center for Research and Advanced Studies, Cinvestav Tamaulipas, Ciudad Victoria 87149, Mexico; grtorres@cinvestav.mx

3 Intelligent Systems Department, Polytechnic University of Victoria, Ciudad Victoria 87138, Mexico; mnunom@upv.edu.mx

* Correspondence: jcaelizondo@docentes.uat.edu.mx

Received: 8 October 2020; Accepted: 30 October 2020; Published: 31 October 2020

Abstract: Distance transform (DT) and Voronoi diagrams (VDs) have found many applications in image analysis. Euclidean distance transform (EDT) can generate forms that do not vary with the rotation, because it is radially symmetrical, which is a desirable characteristic in distance transform applications. Recently, parallel architectures have been very accessible and, particularly, GPU-based architectures are very promising due to their high performance, low power consumption and affordable prices. In this paper, a new parallel algorithm is proposed for the computation of a Euclidean distance map and Voronoi diagram of a binary image that mixes CUDA multi-thread parallel image processing with a raster propagation of distance information over small fragments of the image. The basic idea is to exploit the throughput and the latency in each level of memory in the NVIDIA GPU; the image is set in the global memory, and can be accessed via texture memory, and we divide the problem into blocks of threads. For each block we copy a portion of the image and each thread applies a raster scan-based algorithm to a tile of $m \times m$ pixels. Experiment results exhibit that our proposed GPU algorithm can improve the efficiency of the Euclidean distance transform in most cases, obtaining speedup factors that even reach 3.193.

Keywords: Euclidean distance transform; image processing; CUDA; GPU

1. Introduction

The distance transform is an operator applied, in general, to binary images, composed of foreground and background pixels. The result is an image, called a distance map, with the same size of the input image, but where foreground pixels are assigned a numeric value to show the distance to the closest background pixel, according to a given metrics. Common metrics of distance are city block or Manhattan distance (four-connected neighborhood), chessboard or Tchebyshev distance (eight-connected neighborhood), approximated Euclidean distance, and exact Euclidean distance.

There is a wide variety of applications for the distance transform, including bioinformatics [1], computer vision [2], image matching [3], artistic applications [4], image processing [5], robotics path planning and autonomous locomotion [6], and computational geometry [7].

The distance map for an input image of $n \times n$ pixels can be computed, obviously, in $O(n^4)$ time using brute force. Now, depending on the employed metrics, distance information from the neighborhood of a pixel can be exploited to compute the distance value, and different algorithms have been proposed in order to exploit the local information [2]. In general, the algorithms can be classified in parallel, sequential, and propagation approaches.

Parallel and sequential approaches use a distance mask, placed over every foreground pixel of the input image; the mask size corresponds to the neighborhood size, in order to compute the corresponding distance value. In parallel algorithms, every pixel is continuously refreshed, individually, until no pixel value changes. Thus, the number of iterations is proportional to the largest distance in the image. These algorithms are simple and highly parallelizable.

Sequential algorithms use a raster method, also known as chamfer method, considering that the modification of a distance value on a pixel affects its neighborhood, leading to highly efficient algorithms, which are not parallelizable. In 1966 Rosenfeld and Pfaltz proposed the first sequential Distance transform (DT) algorithms by raster scanning with non-Euclidean metrics [8]. Later, in [9], they proposed city block and chessboard metrics. Borgefors [10] improved the raster scan method and presented local neighborhoods of sizes up to 7×7. Butt and Maragos in [11] present an analysis of the 2D raster scan distance algorithm using mask of 3×3 and 5×5.

Danielsson in [12] proposes the 4SED and 8SED algorithms using four masks of relative displacement pixels. Many improvements have been proposed for Danielsson's algorithm, one is presented in [13] which proposes the signed distance map 4SSED and 8SSED. Leymarie and Levine [14] present an optimized implementation of Danielson's algorithm, obtaining a similar complexity to other chamfer methods. Ragnemalm [15] presents another improvement by means of a separable algorithm for arbitrary dimensions. In [16], Cuisenaire and Macq perform post-processing on Danielson's 4SED algorithm, which allows them to correct any errors that may occur in the distance calculation. In [17], Shih and Wu use a dynamical neighborhood window size and in [18] they use a 3×3 window to obtain the exact Euclidean distance transform.

In [19], Grevera presents the dead reckoning algorithm which, in addition to computing the distance transformation (DT) for every foreground point (x, y) in the image, also delivers a data structure p that stores the coordinates of the closest background pixel—i.e., a Voronoy Diagram (VD) description of the image. This algorithm can produce more accurate results than previous raster scan algorithms.

Paglieroni in [20] and [21] presents independent sequential algorithms, where firstly the distance transform is computed independently for each row of the image to obtain an intermediate result along only one dimension; next, this set of 1D results is used as input for a second phase to obtain the distance transform of the whole image. Another similar approach is presented by Saito and Toriwaki [22] with a four-phase algorithm to obtain the Euclidean distance transform and the Voronoi diagram, by applying n-dimensional filters in a serial decomposition. By exploiting the separable nature of the distance transform and reducing dimensionality, these algorithms can be implemented in parallel hardware architectures as a parallel row-wise scanning followed by a parallel column-wise scanning. However, this restricts the parallelism to only one thread per row and column.

Finally, propagation methods use queue data structures to manage the propagation boundary of distance information from the background pixels, instead of centered distance masks. These algorithms are also very difficult to parallelize. Piper and Granum [23] present a strategy that uses a breadth-first search to find the propagated distance transform between two points in convex and non-convex domains. Verwer et al. [24] use a bucket structure to obtain the constrained distance transform. Ragnemalm [25] uses an ordered propagation algorithm, using a contour set that at first contains only background and adds neighbor pixels, one at a time, until covering the whole image, just as Dijkstra's algorithm does. Eggers [26] avoid extra updates adding a list to Ragnemalm's approach. Sharahia and Christofides [27] treat the image as a graph and solve the distance transformation as the shortest path forest problem. Falcao et al. [28] generalize Sharahia and Christofides' approach to a general tool for image analysis. Cuisenaire and Macq [29] use ordered propagation, producing a first fast solution and then use larger neighborhoods to correct possible errors. Noreen et al. [6] solve the robot path planning problem using a constrained distance transform, dividing the environment in cells and each cell is marked as free or occupied (similar to black and white pixels) and uses an A* algorithm variation to obtain the optimal path.

In recent years, parallel architectures and, particularly, GPU-based architectures are very promising due to their high performance, low power consumption and affordable prices. Recently GPU-based approaches have arisen. Cao et al. in [30] proposed the Parallel Banding Algorithm (PBA) on the GPU to compute the Euclidean distance transform (EDT) and they process the image in three phases. In phase 1, they divide the image into vertical bands and use a thread to handle each band in each of the rows and next propagate the information to a different band. In phase 2, they divide the image into horizontal bands and again use threads for each band and a double-linked list to calculate the proximate sites. Finally, in phase 3, they compute the closest site for each pixel using the result of phase 2. Since a common data structure for potential sites is required among the threads, the implementation of this structure and the coordination of threads is relatively complex in a GPU.

Manduhu and Jones in [31] presented a GPU algorithm in which the operations are optimized using binary functions of CUDA to obtain the EDT in images. They, similar to the PBA algorithm, make a dimensional reduction solving the problem by rows in a first phase, then by columns in a second phase, and finally find the closest feature point for every foreground pixel and compute the distance between them, based on the two previous results.

In [32], the authors present a parallel GPU implementation where they reduce dimensionality. They split the problem into two phases: during the first phase, every column in the image is scanned twice, downwards and upwards, to propagate the distance information; during the second phase, this same process is operated for every row, left-to-right, right-to-left. For its implementation, a CUDA architecture was used, with an efficient utilization of hierarchical memory.

Rong and Tan [33] proposed the Jump Flooding Algorithm (JFA) to compute the Voronoi map and the EDT on GPUs to obtain a high memory bandwidth. They utilize texture units and memory access is regular and coalesced, allowing them to obtain speedup. In [34], Zheng et al. proposed a modification to the JFA [33] to parallelly render the power diagram.

Schneider et al. [35] modify Danielson's algorithm [12] in a sweep line algorithm that was implemented in a GPU. With this approach, distance information can be propagated simultaneously among the pixels within the same row or column, but only one row or column can be processed at a time. In [36], Honda et al. apply a correction algorithm to Schneider et al.'s approach [35] in order to correct errors caused by the vector propagation.

In [37], the authors review PBA [30] implementation and propose some improvements, obtaining the PBA+ algorithm. They show, through new experimentations, that the new PBA+ algorithm provides a better performance than the PBA algorithm. In their website, the authors also share the source code of their algorithm and the appropriate parameters for different GPUs.

In this paper, we present a new parallel algorithm for the computation of the Euclidean distance map of a binary image. The basic idea is to exploit the throughput and the latency in each level of memory in the NVIDIA GPU; the image is set in the global memory, and accessed through texture memory, and we divide the problem into blocks of threads. For each block we copy a portion of image and each thread applies a raster scan-based algorithm to a tile of $m \times m$ pixels.

This document is organized as follows: Section 2 outlines the materials and methods involved in our approach, Parallel Raster Scan for Euclidean Distance Transform (PRSEDT), to compute the Euclidean distance transform for a binary image using a GPU architecture. Section 3 presents some numerical results that show the performance of our method, for different binary images, and these results are compared with the PBA+ algorithm, which is one of the most performing GPU algorithms for computing exact Euclidean distance transform. Finally, in Section 4 we present our conclusions and discussions for future research.

2. Materials and Methods

As stated by Fabbri et al. [2], the distance transform problem can be described as the equation below, given a binary grid Ω of $n \times m$ cells

$$\Omega = \{0, 1, \ldots, n-1\} \times \{0, 1, \ldots, m-1\}$$

that represents the image, on which we can define a binary map I as follows:

$$I : \Omega \rightarrow \{0, 1\}$$

By convention, 0 is associated with black and 1 with white. Hence, we have an object O represented by all the white pixels:

$$O = \{p \in \Omega \big| I(p) = 1\}$$

The set O is called the object or foreground and can consist of any subset of the image domain, including disjoint sets. The elements of its complement, O^c, the set of black pixels in Ω, are called background. We can define the distance transform (DT) as the transformation that generates a map D whose value in each pixel p is the smallest distance from this pixel to O^c:

$$D(p) = \min\{d(p,q) \big| q \in O^c\} = \min\{d(p,q) \big| I(q) = 0\}$$

The Euclidean distance transform $d(p,q)$ is taken as the distance, given by:

$$d(p,q) = \sqrt{(p_x - q_x)^2 + (p_y - q_y)^2}$$

The Voronoi diagram is a partition defined in the domain Ω, based on the linear distance of the sites $VD(p)$. Each Voronoi cell is defined as:

$$VD(p) = \{x \in \Omega \big| d(x, x_i) \leq d(x, x_j);\ x_i, x_j \in O^c \text{ and } i \neq j\}$$

Algorithm 1 shows a sequential raster scan for DT computation based on the Borgefors [10] approach, which consists of initializing the distance map array d to zero for the characteristic pixels and ∞ for the others, and executing a two-phase raster scan for distance propagation with two different scan masks. Each pass employs local neighborhood operations in order to minimize the current distance value assigned to the pixel $C = (x,y)$, located at the center of the mask, by comparing the current distance value with the distance value assigned to each neighbor cell plus the value specified by the mask. Scan masks employed for city block, chessboard, and Euclidean metrics are shown in Figure 1.

Algorithm 1. Sequential Raster Scan DT.

REQUIRE Img—A binary image
ENSURE d—A bidimentional matrix with distances of Img
Initialize d
for y = each line from the top of the Img **then**
  for x = each cell in the line from left to right **then**
    $d(x,y) = \min\{ d(x,y), d(x,y) + C(x-1,y), d(x,y) + C(x-1,y-1), d(x,y) + C(x,y-1),$
      $d(x,y) + C(x+1,y+1)\}$
for y = each line from the bottom of the Img **then**
  for x = each cell in the line from right to left **then**
    $d(x,y) = \min\{ d(x,y), d(x,y) + C(x-1,y+1), d(x,y) + C(x,y+1), d(x,y) + C(x+1,y+1),$
      $d(x,y) + C(x+1,y)\}$

Since it is a separable problem, the exact Euclidean distance problem can be treated by reducing the dimension of the input data [2,20,21]. Exploiting this property, the Euclidean distance problem can be solved efficiently using parallelism in columns and rows [30–32,37]. However, this process requires that each computation thread has access to a complete column of the image, as well as a common

stack structure for the management of potential sites, so its implementation in GPUs and its thread coordination process are relatively complex processes.

The proposed algorithm, called Parallel Raster Scan for Euclidean Distance Transform (PRSEDT), presents a different approach: the image is set in global memory, and can be accessed via texture memory, and is then processed by a grid of processing blocks. Each block is composed of a set of threads and deals with a quadrangular region of the image (CUDA block); in turn, each region is divided into smaller sections (TILES) in which an individual thread applies a raster algorithm for the propagation of the distance transformation. Each thread works independently until no changes are detected in the entire block, so only a boolean value is required to determine if the block has finished processing. The number of iterations is proportional to the size of the block and the maximum distance in the image, and inversely proportional to the number of regions. The resulting algorithm is highly parallelizable, with few synchronization points and less access to regular memory, making it suitable for implementing in modern GPU architectures, which is reflected in better processing times compared to other state-of-the-art algorithms. Figure 2 shows the representation of what is processed in each thread (a TILE), the CUDA blocks, and the grid of threads blocks.

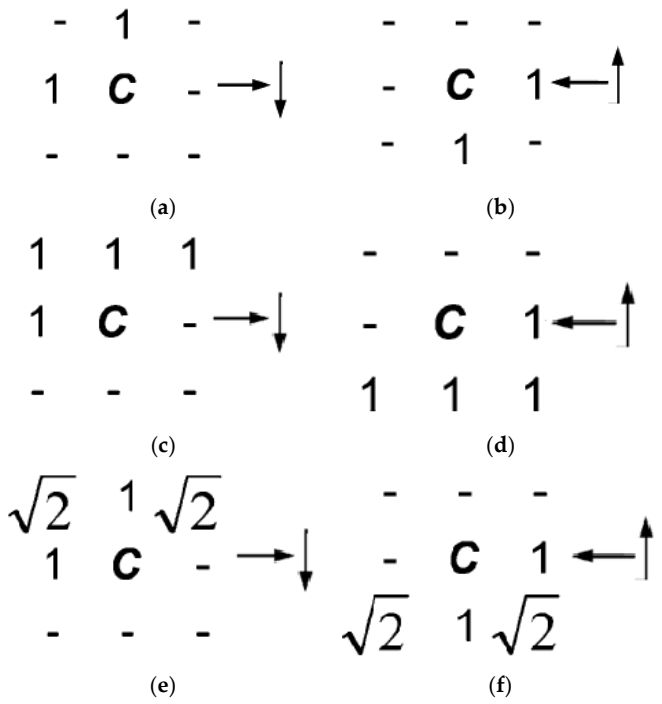

Figure 1. Scan mask metrics. (**a**) City block forward mask; (**b**) city block backward mask; (**c**) chess board forward mask; (**d**) chess board forward mask; (**e**) Euclidean forward mask; (**f**) Euclidean backward mask.

The algorithm processes an input binary image Img (), of $DIM \times DIM$ pixels, to produce the distance map DT and a Voronoi map VD containing, for each pixel, the coordinates of the closest characteristic point; both arrays are the same size as the input image. Initially, the array DT is initialized to zero for the characteristic pixels and ∞ for the others, while the array VD is initialized with the characteristic points pointing to themselves and the other cells without an assigned point, as indicated in Equations (1) and (2).

$$DT(x,y) = \begin{cases} \infty, & Img(x,y) = white \\ 0, & Img(x,y) = black \end{cases} \quad (1)$$

$$VD(x,y) = \begin{cases} NULL, & Img(x,y) = white \\ (x,y), & Img(x,y) = black \end{cases} \quad (2)$$

For processing, the image is divided into $k \times l$ blocks, called CUDA blocks. In turn, each block is divided into $n \times n$ tiles that will be processed in parallel by the threads. This scheme guarantees coalesced access to global memory (for writing data) and texture memory (for reading data), improving processing times.

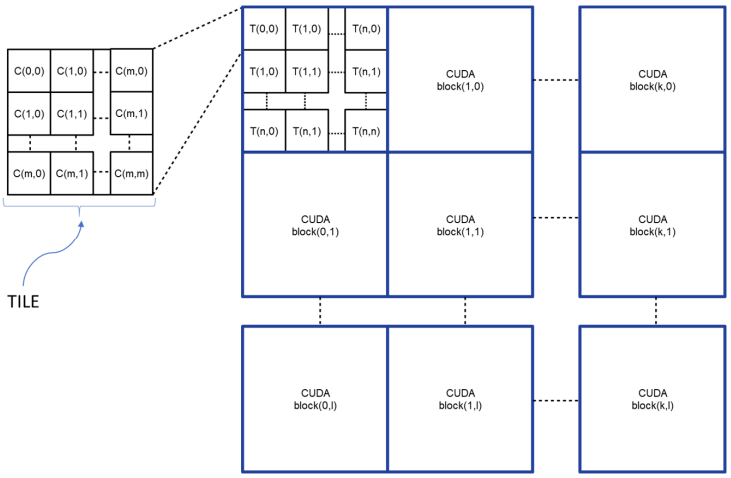

Figure 2. Grid of thread blocks. The block(*k*,*l*) represents each block of CUDA; a block of CUDA contains a number of threads, *T*(*n*,*n*), and a thread process a TILE; each cell of TILE *C*(*x*,*y*) represents a pixel of the input image.

For each tile, a processing thread executes a sequential raster distance propagation algorithm, similar to the chamfer method (Algorithm 1), using mask 1 (Figure 3a) in forwards pass (from left to right, top to bottom) and mask 2 (Figure 3b) in backward pass (from right to left, bottom to top). Both masks only indicate the neighbor pixels that will be considered to update the distance value of the cell $r = (x, y)$ under consideration. For each of the neighbor pixels indicated by the mask, it is verified whether if the distance from cell r to the pixel pointed by the neighbor is less than the current recorded distance value. If it is true, the matrix DT is updated with the new distance value, and the matrix VD is updated with the identified characteristic point. The above is summarized with Equations (3) and (4).

$$DT(r) = min\begin{cases} DT(r) \\ \|r - VD(v_i) \end{cases} \tag{3}$$

$$VD(r) = \begin{cases} VD(v_i), & \|r - VD(v_i)\| < DT(r) \\ VD(r), & \|r - VD(v_i)\| \geq DT(r) \end{cases} \tag{4}$$

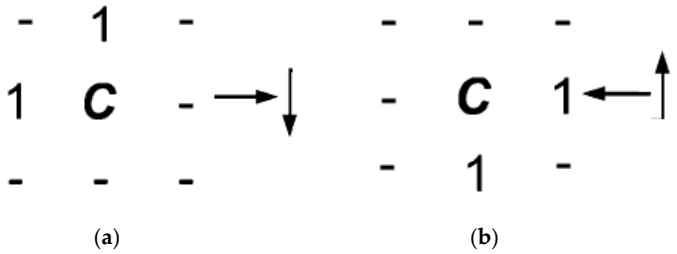

(**a**) (**b**)

Figure 3. Scan masks used in Parallel Raster Scan for Euclidean Distance Transform (PRSEDT). (**a**) Raster scan mask 1, forward pass, from left to right, top to bottom; (**b**) raster scan mask 2, backward pass, from right to left, bottom to top.

Rasters on each tile are performed continuously until changes are no longer detected in both DT and VD arrays. The scan masks used in PRSEDT are shows in Figure 3.

Both the size of the tile and the size of the CUDA block are parameters that were determined experimentally, according to the size of the input image and the architecture of the video card, to obtain the best processing time. The maximum size is given by the parameter m, which indicates the tile size—i.e., the number of pixels that each thread must process (m^2 pixels). The CUDA block size is determined by the parameter n, which determines the number of threads processing a CUDA block (n^2 threads). In this way, the dimensions of the subimage, which is processed in each CUDA block, are $(n \times m + 2)^2$ pixels. The two extra pixels ensure an overlap of one pixel with neighbor blocks to allow the propagation of distance information generated in the block.

To guarantee the proper treatment of the whole input image Img, an array OB of $k \times l$ cells (one cell for each CUDA block) is also used to indicate if each image CUDA block needs to be processed again to update the distance information. The values for the k and l parameters are obtained directly from the dimensions of the input image Img, the size of the CUDA block n, and the number of threads per block m (tile resolution).

The proposed method is divided into two algorithms. The Algorithm 2 Main PRSEDT, is in charge of reading the image and copying it to the global memory of the device, invoking the kernel that initializes the DT, VD and OB arrays, and determining the number of CUDA blocks and threads per block according to the parameters n and m. Next, it invokes the PRSEDTKernel algorithm (Algorithm 3), to propagate the distance information using parallel computing over the CUDA blocks, as many times as necessary, as long as there are changes in the DT and VD arrays.

Algorithm 2. Main PRSEDT

```
REQUIRE  Img—A binary image
ENSURE   DT—A bidimentional matrix with distances of Img
         VD—The voronoi diagram of Img
         cudaMemcpy(VD, Img, cudaMemcpyHostToDevice)//copy Img from Host to Device
         blocks = (DIM/n, DIM/n)//Grid dimensions
         threads = (n, n)//Block dimensions
         initKernel<<blocks, threads>>(DT, VD, OB)//Init DT Equation (1), VD Equation (2) and OB
         blocks = (DIM/( n × m),DIM/( n × m))//Grid dimensions
         threads = (n,n)//Block dimensions
         cudaBindTexture(VD_Tex, VD) ;//Bind the VD in global memory to VD_Tex in texture
         cudaBindTexture(DT_Tex, DT) ;//Bind the VD in global memory to VD_Tex in texture
         cudaBindTexture(OB_Tex,OB) ;//Bind the VD in global memory to VD_Tex in texture
         count ← 1
         ctrl ← 1
         repeat
             flag ← false//use memSet to set false the flag of the device
             blocks(DIM/( n × m),DIM/( n × m))//Grid dimensions
             threads(n, n)//Block dimensions
             PRSEDTKernel <<blocks,threads>>(DT, VD, OB, flag, ctrl)
             count ← count + 1
             if count > 2 then
                 ctrl ← ((count − 2) × n × m/2)^2
             else
                 ctrl ← count^2
             Use cudaMemcpy to copy back the flag from device to host
         until !flag
         float *DT_Host = (float*)malloc(imageSize);
         cudaMemcpy(DT_Host, DT, cudaMemcpyDeviceToHost);
         int *VD_Host = (int*)malloc(imageSize);
         cudaMemcpy(VD_Host, VD, cudaMemcpyDeviceToHost);
```

Algorithm 3.

```
PRSEDTKernel (*DT, *VD, *OB, *flag, *ctrl)
    __shared__ bool shOpt
    __shared__ int optimized
    int optreg ← 0
    if threadIdx.x == 0 AND threadIdx.y == 0 then
        optimized ← 0
        shOpt ← false
        if OB_Tex[blockIdx.x + blockIdx.y * gridDim.x] == 1 then
            shOpt ← true
    syncthreads();
    if shOpt then
        return
    shared float memC[n × m][n × m]
    shared int ptr[n × m + 2][n × m + 2]
    shared bool shEnter;
    memC ← DT_Tex TILE of m^2 (access in a coalesced form)
    for each cell in TILE of memC
        if memC_cell ≤ ctrl then
            optreg + +
    atomicAdd(optimized, optreg)
    syncthreads()
    if optimized == (n × m)^2 then
        OB[blockIdx.x + blockIdx.y × gridDim.x] ← true
        return
    ptr ← VD_Tex TILE of (n × m + 2)^2 (access in a coalesced form)
    repeat
        syncthreads();
        if threadIdx.y == 0 and threadIdx.x == 0 then
            shEnter ← false
        syncthreads();
        for each line from the top of the TILE then
            for each cell in the line of the TILE from left to right then
                apply scan mask 1 (Figure 3a)
                evaluate memC and ptr according to Equations (3) and (4).
                if any update is made then
                    shEnter ← true
        for each line from the bottom of the TILE then
            for each cell in the line of the TILE from right to left then
                apply scan mask 2 (Figure 3b)
                evaluate memC and ptr according to Equations (3) and (4).
                if any update is made then
                    shEnter ← true
        syncthreads()
    until !shEnter
    if any change in the TILE then
        update DT with corresponding TILE of memC
        update VD with corresponding TILE of ptr
        flag ← true
```

The PRSEDTKernel algorithm, shown in Algorithm 3, handles the parallel processing of the CUDA blocks. Initially, the first thread of each block checks if the assigned block requires updating, using the array *OB*. If the block requires no processing, the entire block ends. If processing is required, an array *memC* is created in the shared memory space, and each thread of the block makes a copy of the

distance map *DT* of its respective tile, through a coalesced access to texture memory. Next, the threads of the block verify if, for each cell within its respective tile, the distance value is less than a threshold value *ctrl* (which increases according to the number of iterations, in Algorithm 2 Main PRSEDT). If this condition is verified for all the pixels of the block, then the block is considered as optimized and does not require to be processed again, so the corresponding cell in the array *OB* is updated and the complete block ends.

If the distance map of this block can still be improved, then each thread makes a copy of its respective tile of the Voronoi diagram *VD*, from the texture memory to the shared array *ptr*, with coalesced memory access. From this moment, each thread propagates the distance information in its respective tile, using the sequential raster process described above, until all the threads no longer generate changes.

Finally, if any changes were made to the block, then the *DT* and *VD* arrays in global memory are updated, with the data stored in the arrays *memC* and *ptr* in the block's shared memory. Figure 4 shows a flowchart of the heterogeneous programming model used in PRSEDT: on the left side we can see the process running in host, and on the right side the processes running in device, in order to show the whole coordination of our approach. Briefly, the host is in charge of reading the image and copying it to the global memory of the device, instantiating the kernels and copying back the Voronoi diagram and the distance transform; the device, on the other hand, is in charge of initializing the Voronoi diagram, the distance transform map, and the array OB (initKernel); finally, each thread of PRSEDTKernel processes a tile of VD and DT.

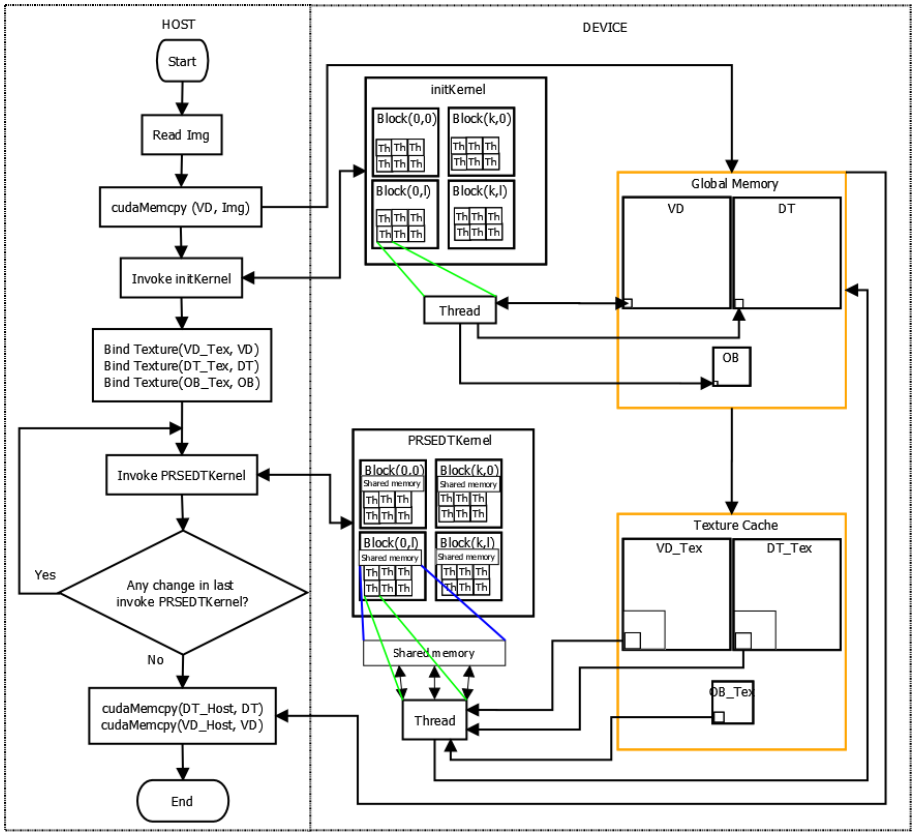

Figure 4. Flowchart of the heterogeneous programming of PRSEDT.

3. Results

For experimentation purposes, the implementation of the proposed algorithm was carried out in a desktop computer equipped with an Intel Core i7-7700 processor, with eight cores at 3.6 GHz,

and an NVIDIA GeForce GTX 1070 video card. The operating system used is Ubuntu 18.04 LTS 64-bit, and the programming language is C++ with CUDA 10.2. We used a NVIDIA "Visual Profiler" to obtain information about the data transfer between the device memory and the host memory, as well as the computation performed by the GPU card.

To evaluate the proposed method, the decision was made to compare it with the PBA+ [37] algorithm, an updated revision of the PBA algorithm [29]. The original PBA algorithm proved to be highly competitive compared to the two most representative state-of-the-art algorithms: Schneider et al.'s [33] and JFA [32]. In its PBA+ version, the authors have achieved significant improvements to the implementation of their original algorithm, with better processing times. In addition, on their website, the authors generously share the source code of their implementation, as well as the recommended values of the different parameters of their algorithm, according to the characteristics of the input image and the video card used. Due to these two factors, we consider that the PBA+ algorithm is a representative state-of-the-art algorithm in the calculation of the distance map in parallel hardware architectures.

It is important to highlight that the distance maps obtained by the PBA+ algorithm and our proposed algorithm (PRSEDT) are exactly the same for all the input images used in experimentation, so the difference between both algorithms is in the performance at runtime and not in the precision of the obtained distance map.

Table 1 shows the parameters proposed by the authors of the PBA+ algorithm for different image resolutions and the GPU card used in this experimentation, where m1, m2 and m3 are the parameters of each phase in the PBA+ algorithm. On the other hand, Table 2 shows the parameters used for our proposed method (PRSEDT), for different image resolutions, obtained by own experimentation.

Table 1. Parameters for the improved Parallel Banding Algorithm (PBA+).

Texture Size	m1	m2	m3
512 × 512	8	16	8
1024 × 1024	16	32	8
2048 × 2048	32	32	8
4096 × 4096	64	32	4
8192 × 8192	64	32	4
16,384 × 16,384	128	32	4

Table 2. Parameters for PRSEDT. m is tile resolution and n is the block size.

Texture Size	TILERES	BSIZE
512 × 512	2	8
1024 × 1024	2	8
2048 × 2048	2	8
4096 × 4096	4	8
8192 × 8192	4	8
16,384 × 16,384	4	8

In order to evaluate the impact of memory transfers from host to device and vice versa, we carried out a set of experiments from which we obtained the transfer time. From Table 3 it can be noted that the transfer time is affected only by the dimensions of the image and is similar for both PRSEDT and PBA+ algorithms. Therefore, in the next experiments, we focus on evaluating the processing time of the algorithms.

Table 3. Memory transfer times (milliseconds). Column HostToDevice indicates the transfer time of the image from the host to the device, while the DeviceToHost columns indicate the transfer time from the device to the host of the Distance transform (DT) and Voronoi diagram (VD) matrices, respectively.

Texture Size	PRSEDT			PBA+		
	HostToDevice	DeviceToHost		HostToDevice	DeviceToHost	
512 × 512	0.082	0.08042	0.0881	0.082	0.0809	0.0811
1024 × 1024	0.598	1.31	1.28	0.593	1.28	1.27
2048 × 2048	2.7979	6.49	6.56	2.91	6.35	6.19
4096 × 4096	12.11	26.95	26.93	12.1	26.79	26.68
8192 × 8192	49.5	108.64	108.89	48.8	108.72	109.01
16,384 × 16,384	191.63	438.94	439.01	194.01	438.61	438.5

In the first phase of experimentation, the performance of the algorithms for input images of different resolutions and with different densities of randomly generated feature points was compared. The density of random feature points took values of 1%, 10%, 30%, 50%, 70% and 90%, with resolutions of 512 × 512, 1024 × 1024, 2048 × 2048, 4096 × 4096, 8192 × 8192 and 16384 × 16384. Figure 5 shows an example of the set of images of 1024 × 1024 pixels of resolution, for different density values.

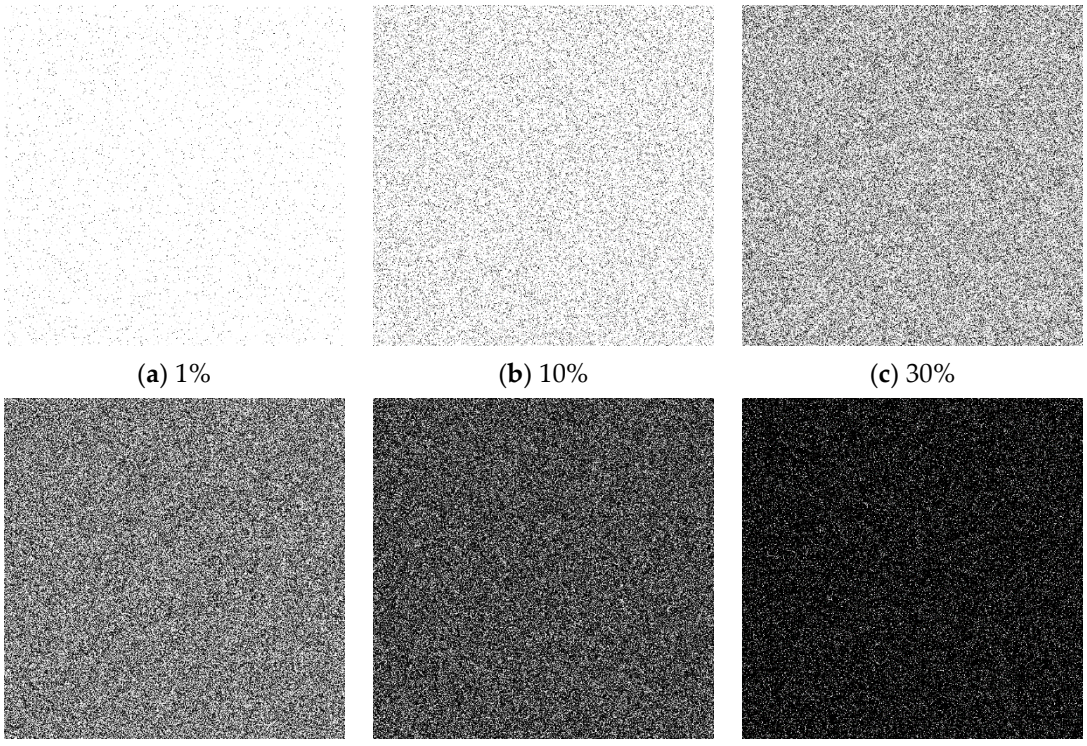

(**a**) 1% (**b**) 10% (**c**) 30%

Figure 5. Input images with different densities of black pixels (1024 × 1024). (**a**) 1%; (**b**) 10%; (**c**) 30%; (**d**) 50%; (**e**) 70%; (**f**) 90%.

Table 4 shows the processing time in milliseconds and the speedup factor obtained for images of different densities and resolutions. In 512 × 512 resolution images, the PRSEDT improves the performance of the PBA+ algorithm in all cases, with speedup factors ranging from 1.044 for 1% density images to 3.441 for images with 90% density.

Table 4. Running time (milliseconds) of each image with different densities of black pixels and different resolutions.

Density	Algorithm	512 × 512		1024 × 1024		2048 × 2048	
		ms	Speedup	ms	Speedup	ms	Speedup
1%	PBA+	0.335	1.044	0.801	0.803	2.545	0.745
	PRSEDT	0.321		0.998		3.415	
10%	PBA+	0.38	1.827	0.968	1.763	3.111	1.590
	PRSEDT	0.208		0.549		1.956	
30%	PBA+	0.41	2.343	1.066	2.406	3.214	2.169
	PRSEDT	0.175		0.443		1.482	
50%	PBA+	0.408	2.684	1.074	3.294	3.181	3.233
	PRSEDT	0.152		0.326		0.984	
70%	PBA+	0.395	3.110	1.034	3.517	2.996	3.428
	PRSEDT	0.127		0.294		0.874	
90%	PBA+	0.382	3.441	0.985	3.717	2.87	3.470
	PRSEDT	0.111		0.265		0.827	
Density	**Algorithm**	**4096 × 4096**		**8192 × 8192**		**16, 384 × 16, 384**	
		ms	**Speedup**	**ms**	**Speedup**	**ms**	**Speedup**
1%	PBA+	8.89	0.800	30.49	0.881	117.87	0.865
	PRSEDT	11.11		34.61		136.24	
10%	PBA+	10.25	1.253	36.13	1.401	136.95	1.363
	PRSEDT	8.18		25.79		100.5	
30%	PBA+	10.21	1.383	36.94	1.564	139.28	1.481
	PRSEDT	7.38		23.62		94.04	
50%	PBA+	9.93	2.315	35.82	2.588	135.99	2.508
	PRSEDT	4.29		13.84		54.23	
70%	PBA+	9.44	2.275	34.06	2.604	130.15	2.503
	PRSEDT	4.15		13.08		52	
90%	PBA+	9.01	2.346	32.78	2.646	121.08	2.478
	PRSEDT	3.84		12.39		48.86	

For 1024×1024 pixel resolution images, the PBA+ algorithm performs better on 1% density images, but our PRSEDT algorithm achieves better results for images with 10% to 90% density, with speedup factors ranging from 1.763 to 3.717.

In the case of 2048×2048 resolution images with 1% density, the speedup factor was 0.745, so the PBA+ algorithm obtains better results than PRSEDT; however, for densities from 10% to 90%, our algorithm performs better, with speedup factors ranging from 1.590 to 3.470.

For images with a resolution of 4096×4096 pixels, the performance pattern is repeated: for 1% density there is a speedup factor of 0.800, and the PBA+ algorithm obtains better results than our method. Nevertheless, for densities from 10% up to 90%, the proposed method performs better, with speedup factors ranging from 1.253 to 2.346.

With 8192×8192 resolution images, we obtained a speedup factor of 0.881 for a density of 1%, and for densities from 10% to 90%, the speedup factor ranges from 1.401 to 2.646.

Finally, for images with a resolution of $16,384 \times 16,384$, the obtained speedup factor for 1% density is 0.865, while for densities of 10%, 30%, 50%, 70% and 90%, the speedup factors are 1.363, 1.481, 2.508, 2.503 and 2.478, respectively.

From the data of Table 3, we can see that in 31 out of the 36 cases PRSEDT yields better results than the PBA+. The better performance of PBA+ in low-density images can be explained because, as mentioned above, the number of iterations of the proposed method is proportional to the maximum image distance, which is greater in very low-density images. However, it can be observed that in most cases (21 out of 36) a speedup factor greater than 100% is obtained, even tripling the performance of the PBA+ algorithm in some cases.

Figure 6 shows an example of the results obtained for an input image with random feature points (Figure 6a) with the grayscale distance map (Figure 6b) and the Voronoi diagram (Figure 6c).

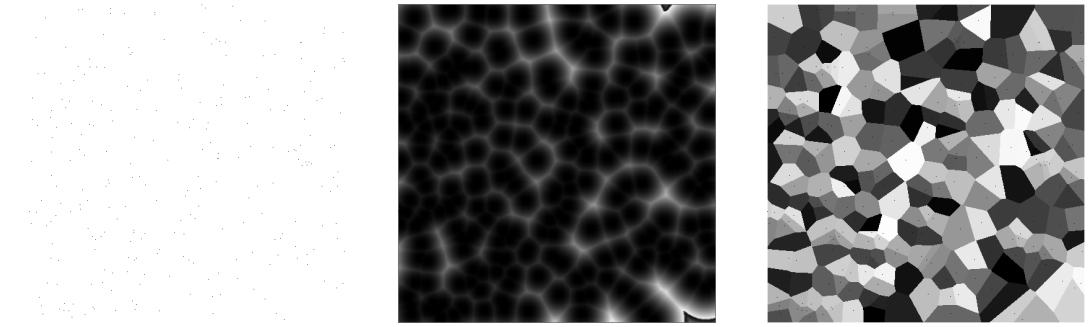

(**a**) (**b**) (**c**)

Figure 6. Example of distance transform and Voronoi diagram for an input image with random features. (**a**) Input image with 0.1% density of black pixels; (**b**) grayscale distance map, the color gradient is caused by the color table, to better visualize the distances; (**c**) Voronoi diagram.

Table 5 shows, for each resolution and for each density of black pixels, the number of times the PRSEDTKernel was instantiated. As can be seen, the higher the density the fewer instances needed, which is related to the maximum value in the distance map. Figure 7 shows the timeline of the execution of the PRSEDT algorithm and the PBA+ algorithm for an input image of 2048 × 2048 pixels and a density of 30%. On the one hand, our PRSEDT algorithm instance only has two kernels: the initKernel for initialization of DT and VD matrices, and the PRSEDTKernel three times (Figure 7a) for distance propagation. On the other hand, the PBA+ algorithm requires instantiating 10 different kernels, making its implementation more complex (Figure 7b).

Table 5. PRSEDTKernel instances.

Density	512 × 512	1024 × 1024	2048 × 2048	4096 × 4096	8192 × 8192	16, 384 × 16, 384
1%	4	4	5	4	4	4
10%	3	3	3	3	3	3
30%	3	3	3	3	3	3
50%	3	3	3	3	3	3
70%	2	2	2	3	3	3
90%	2	2	2	3	3	3

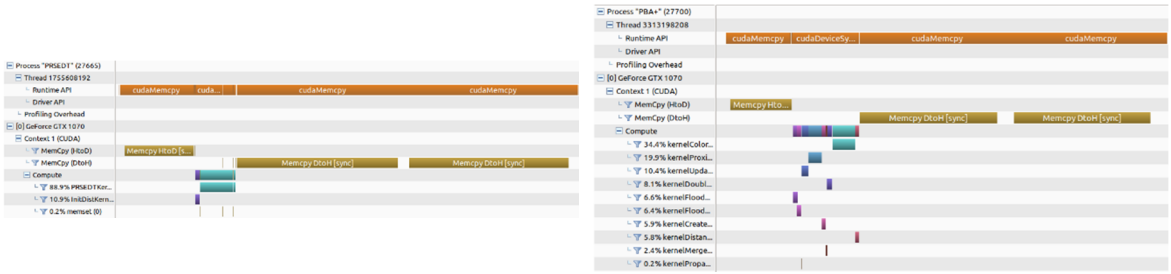

(**a**) (**b**)

Figure 7. Timelines for an input image for 2048 × 2048 pixels and 30% density, showing memory data transfers and computing times. (**a**) PRSEDT profiling; (**b**) PBA+ profiling.

In the second phase of experimentation, the performance of the proposed algorithm for specific binary images was verified. The Lena, Mandril and Retina images were taken as input images

(Figure 8), with resolutions of 512×512, 1024×1024, 2048×2048, 4096×4096, 8192×8192 and $16,384 \times 16,384$ pixels. The results are summarized in Table 6, with the execution time in milliseconds and the speedup factor with respect to the PBA+ algorithm for each of the images.

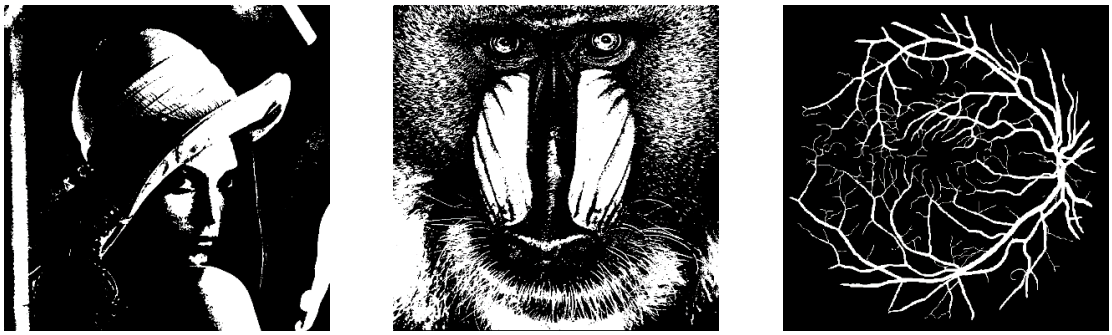

(**a**) (**b**) (**c**)

Figure 8. Input images. (**a**) Lena; (**b**) Mandril; (**c**) Retina.

Table 6. Running time (milliseconds) of each image with different input images and different resolutions.

Image	Algorithm	512 × 512		1024 × 1024		2048 × 2048	
		ms	Speedup	ms	Speedup	ms	Speedup
Lena	PBA+	0.401	1.604	1.029	1.790	2.87	1.535
	PRSEDT	0.25		0.575		1.87	
Mandril	PBA+	0.434	1.507	1.074	1.554	2.99	1.187
	PRSEDT	0.288		0.691		2.52	
Retina	PBA+	0.402	2.871	0.993	3.193	2.82	3.099
	PRSEDT	0.14		0.311		0.91	
Image	**Algorithm**	**4096 × 4096**		**8192 × 8192**		**16,384 × 16,384**	
		ms	**Speedup**	**ms**	**Speedup**	**ms**	**Speedup**
Lena	PBA+	8.68	1.072	29.69	1.107	116.93	0.809
	PRSEDT	8.1		26.82		144.51	
Mandril	PBA+	9.24	0.857	30.81	0.812	116.66	0.566
	PRSEDT	10.78		37.94		206.29	
Retina	PBA+	8.72	2.047	30.24	2.625	114.24	2.587
	PRSEDT	4.26		11.52		44.16	

Table 7 shows, for each resolution and input image from Figure 8, the number of times that the PRSEDTKernel was instantiated. Since the Mandril and Lena input images have wider white areas, the maximum distance value is greater than in the Retina image. This fact is reflected in the greater number of instantiations required of the PRSEDTKernel to propagate the distance information among tiles and CUDA blocks in these large white areas, thus delaying the propagation of the distance transformation. The Retina image requires fewer instances due to smaller areas of white pixels.

Table 7. Number of PRSEDTKernel instances required to process the input image.

Image	512 × 512	1024 × 1024	2048 × 2048	4096 × 4096	8192 × 8192	16, 384 × 16, 384
Lena	5	8	14	15	27	51
Mandril	6	8	14	14	28	54
Retina	3	4	5	5	7	11

For the Lena image (Figure 8a), it can be seen that the proposed algorithm improves the performances of the PBA+ algorithm by a factor of 1.604 for the 512×512 resolution, 1.790 for the

1024 × 1024 resolution, 1.535 for the 2048 × 2048 resolution, 1.072 for the 4096 × 4096 resolution and finally 1.107 for 8192 × 8192 resolution. In the case of the 16,384 × 16,384 resolution, the PBA+ algorithm showed a better performance, with a speedup factor of 0.809. Figure 9 shows the resulting distance map and Voronoi diagram for the 2048 × 2048-pixel Lena image.

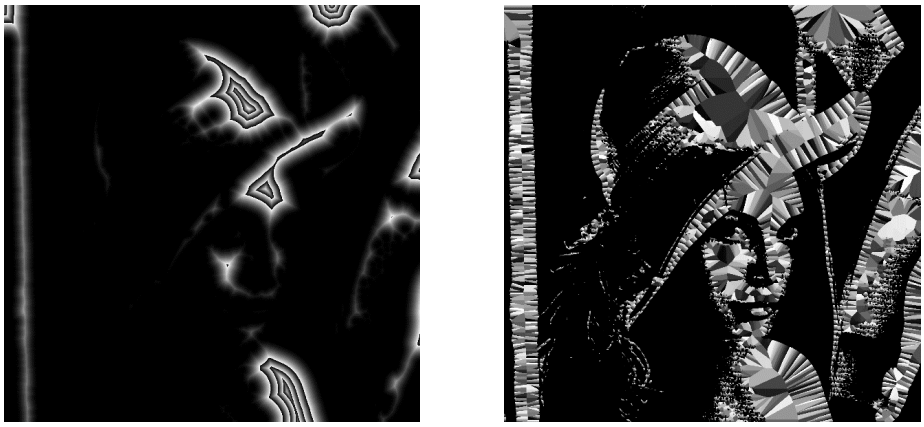

(**a**) (**b**)

Figure 9. Results obtained from Lena input image for the 2048 × 2048-pixel image. (**a**) Gray scale distance map, the color gradient is caused by the color table, to better visualize the distances; (**b**) Voronoi diagram.

Figure 10 shows the timelines for the PRSEDT algorithm and the PBA+ algorithm, while processing the Lena input image of 2048 × 2048 pixels. The PRSEDT algorithm (Figure 10a) is required to instantiate the PRSEDTkernel 14 times (as reported in Table 6), each instantiation requiring a reset of the global flag at the beginning and a memcopy from the device to host to verify the result of the flag at the end of the PRSEDTKernel execution. The times required for these data transfers are considered in the total processing time. On the other hand, the PBA+ algorithm does not require additional memory data transfers between host and device; however, the total processing time is higher than our approach (Table 6).

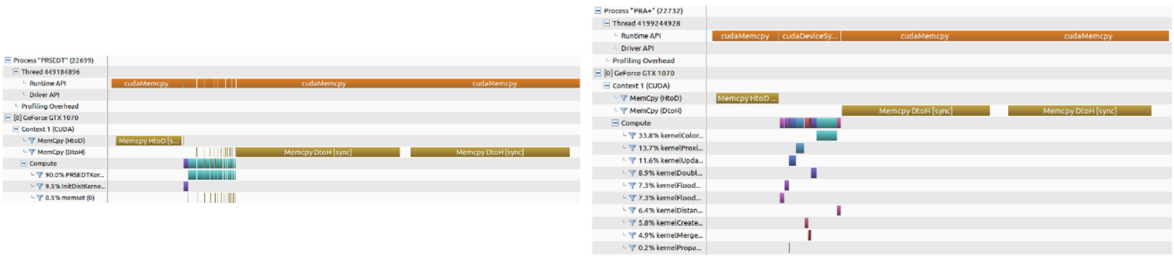

(**a**) (**b**)

Figure 10. Timelines for 2048 × 2048-pixel Lena input image, showing memory data transfers and computing times. (**a**) PRSEDT profiling; (**b**) PBA+ profiling.

For the Mandril image (Figure 8b), it can be seen that our proposal improves the performance of the PBA+ algorithm in resolutions of 512 × 512, 1024 × 1024, and 2048 × 2048 pixels, with speedup factors of 1.507, 1.554, and 1.187, respectively. The PBA+ algorithm showed better results for the resolutions of 4096 × 4096, 8192 × 8192, and 16,384 × 16,384 pixels, with speedup factors of 0.857, 0.812 and 0.566, respectively. The results obtained for the 2048 × 2048-pixel image are shown in Figure 11.

Figure 12 shows the timeline of the execution of the PRSEDT algorithm and the PBA+ algorithm for the 2048 × 2048 pixels Mandril input image. As for the Lena image, we can see in Figure 12a that PRSEDT algorithm requires to instantiate 14 times the PRSEDTkernel (Table 6) to process the whole

image, with their respective memory data transfers of the flag value between the Host and the Device. However, the total processing time is lower than the PBA+ algorithm (Figure 12b).

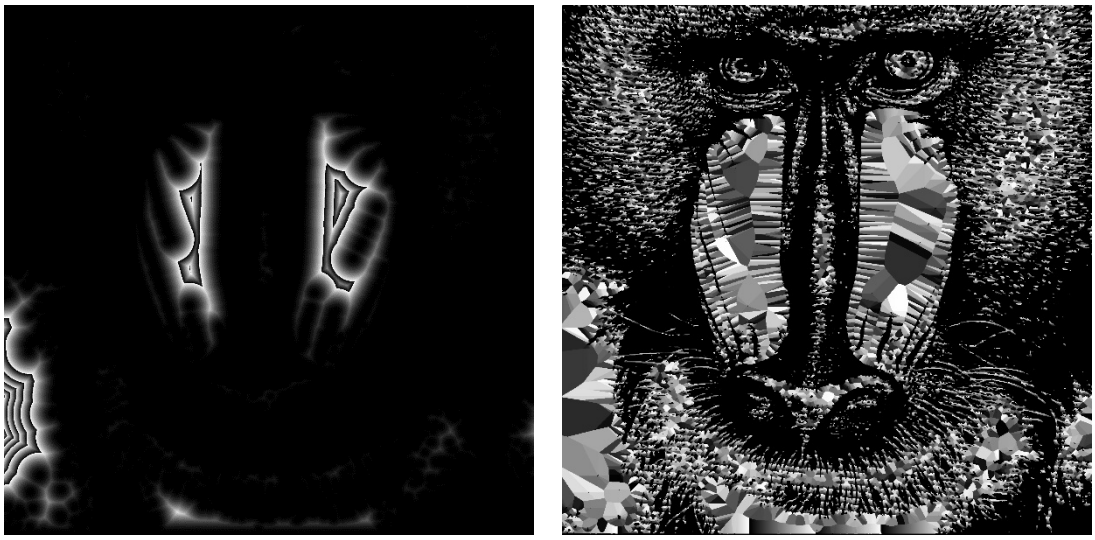

(**a**) (**b**)

Figure 11. Results obtained from Mandril input image for the 2048 × 2048-pixel image. (**a**) Gray scale distance map, the color gradient is caused by the color table, to better visualize the distances; (**b**) Voronoi diagram.

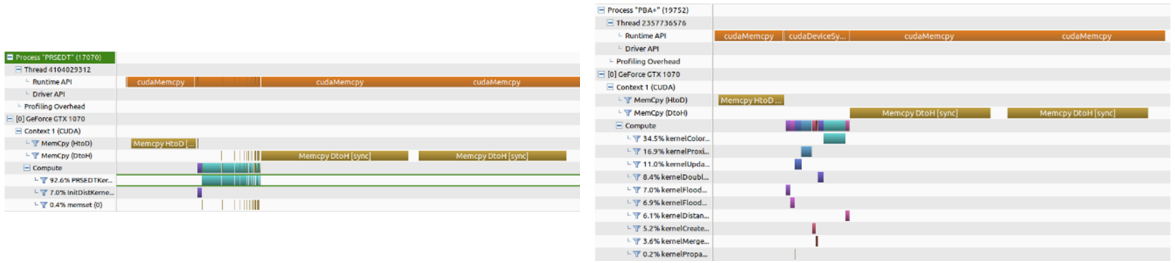

(**a**) (**b**)

Figure 12. Timeline from Mandril input image for the 2048 × 2048-pixel image showing memory copy and computing times. (**a**) PRSEDT profiling; (**b**) PBA+ profiling.

Finally, for the Retina image (Figure 8c), the proposed method improves the performance of the PBA+ algorithm in all cases, with speedup factors of 2.871 for the resolution of 512 × 512, of 3.193 in the image of 1024 × 1024 pixels, of 3.099 for the resolution of 2048 × 2048, of 2.047 for the resolution of 4096 × 4096, of 2.625 for the 8192 × 8192-pixel image, and for a resolution of 16, 384 × 16, 384 pixels the execution time was improved by 2.587. The results obtained for the Retina image and 2048 × 2048-pixel image are shows in Figure 13.

Figure 14 shows the profiles of the PRSEDT algorithm and the PBA+ algorithm while processing the 2048 × 2048-pixel Retina input image. Since this image has smaller white areas, the PRSEDT algorithm only requires five instances of the PRSEDTkernel to process the image. This image shows the true potential of our algorithm: a simpler algorithm can outperform a more complex algorithm.

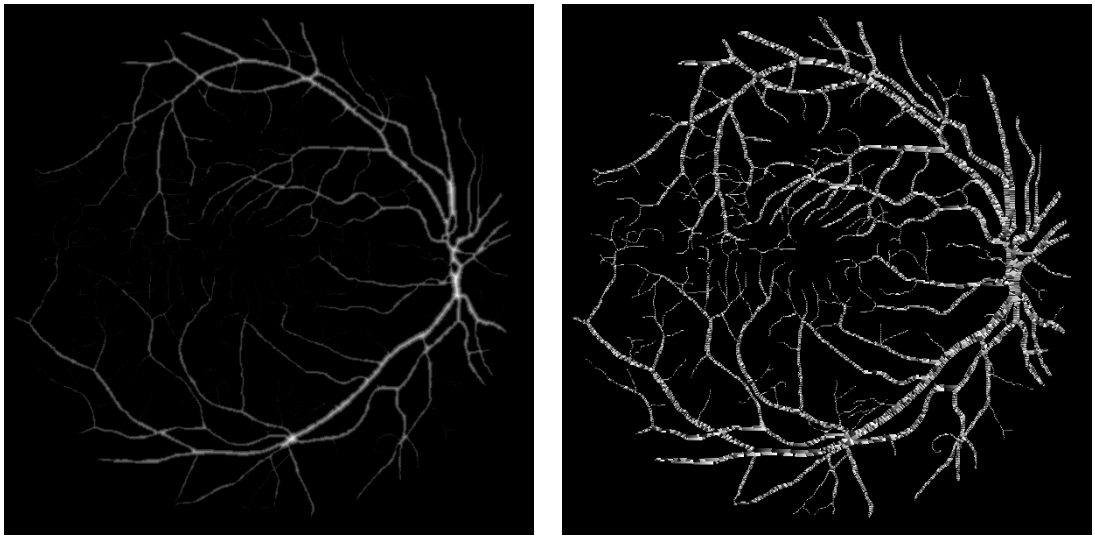

(**a**) (**b**)

Figure 13. Results obtained from Retina input image for the 2048 × 2048-pixel image. (**a**) Gray scale distance map, the color gradient is caused by the color table, to better visualize the distances; (**b**) Voronoi diagram.

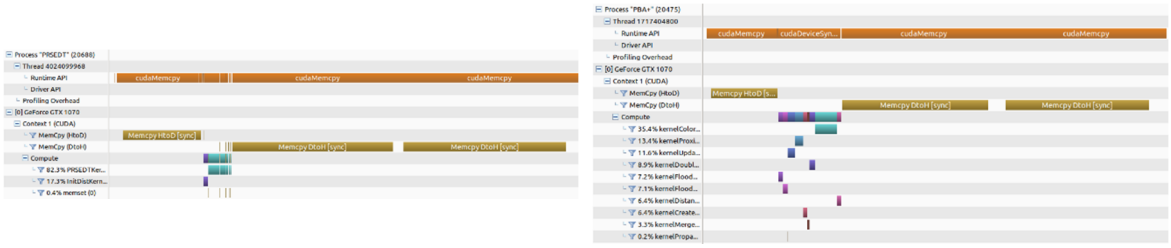

(**a**) (**b**)

Figure 14. Timelines for the 2048 × 2048-pixel Retina input image, showing memory data transfers and computing times. (**a**) PRSEDT profiling; (**b**) PBA+ profiling.

4. Conclusions

In this document, a new parallel algorithm is proposed for the computation of the exact Euclidean distance map of a binary image. In this algorithm, a new approach is proposed that mixes CUDA multi-thread parallel image processing with a raster propagation of distance information over small fragments of the image. The way in which these image fragments are organized, as well as the coalesced access to global and texture memory, allow better use of the architecture of modern video cards, which is reflected in the better processing times, both in small and large images.

The PBA algorithm, in 2010, turned out to be a much more competitive algorithm than the other state-of-the-art approaches at the time. Even now, the PBA algorithm is a reference in the literature of the research area. On their website, the authors of the PBA+ algorithm show that this variant is faster than the original algorithm, significantly improving its performance in all cases, particularly in large-size images with a significant density of feature points.

Therefore, together with the possibility of directly obtaining the source code of this algorithm, we decided to use the PBA+ algorithm as a reference control to evaluate the proposed approach's performance.

From the experimentation carried out, we can verify that, in most cases, the proposed algorithm performs better than the PBA+ algorithm, obtaining speedup factors that even reach 3.193—that is,

they divide the required processing time by three. There are some situations where the PBA+ algorithm is better, particularly in images where the largest distance value is relatively large, which occurs in high-resolution images with a low density of feature points. Even in these cases, the performance loss of our algorithm is around 20% only in most cases.

Author Contributions: Conceptualization, J.C.E.-L. and J.G.R.-T.; formal analysis, J.H.B.-Z. and M.A.N.-M.; funding acquisition, V.P.S.-A.; investigation, J.C.E.-L., J.G.R.-T., J.H.B.-Z. and A.D.-M.; methodology, J.C.E.-L., J.H.B.-Z. and V.P.S.-A.; project administration, J.C.E.-L. and J.G.R.-T.; software, J.C.E.-L., J.H.B.-Z. and A.D.-M.; supervision, J.G.R.-T. and A.D.-M.; validation, J.C.E.-L., A.D.-M. and V.P.S.-A.; writing—original draft, J.G.R.-T., A.D.-M., M.A.N.-M. and V.P.S.-A.; writing—review and editing, J.C.E.-L., J.H.B.-Z. and M.A.N.-M. All authors have read and agreed to the published version of the manuscript.

Funding: The APC was funded by Facultad de Ingeniería y Ciencias, Universidad Autónoma de Tamaulipas.

Conflicts of Interest: The authors declare no conflict of interest.

References

1. Lo Castro, D.; Tegolo, D.; Valenti, C. A visual framework to create photorealistic retinal vessels for diagnosis purposes. *J. Biomed. Inform.* **2020**, *108*, 103490. [CrossRef] [PubMed]
2. Fabbri, R.; Costa, L.D.F.; Torelli, J.C.; Bruno, O.M. 2D Euclidean distance transform algorithms: A comparative survey. *ACM Comput. Surv.* **2008**, *40*, 1–44. [CrossRef]
3. Ghafoor, A.; Iqbal, R.N.; Khan, S. Image matching using distance transform. In *Image Analysis*; Bigun, J., Gustavsson, T., Eds.; Springer: Berlin/Heidelberg, Germany, 2003; Volume 2749, pp. 654–660. ISBN 9783540406013.
4. de Berg, M.; van Kreveld, M.; Overmars, M.; Schwarzkopf, O.C. *Computational Geometry: Algorithms and Applications*; Springer: Berlin/Heidelberg, Germany, 2000; ISBN 9783662042472.
5. Arcelli, C.; di Baja, G.S.; Serino, L. Distance-Driven Skeletonization in Voxel Images. *IEEE Trans. Pattern Anal. Mach. Intell.* **2011**, *33*, 709–720. [CrossRef]
6. Noreen, I.; Khan, A.; Asghar, K.; Habib, Z. A Path-Planning Performance Comparison of RRT*-AB with MEA* in a 2-Dimensional Environment. *Symmetry* **2019**, *11*, 945. [CrossRef]
7. Lam, L.; Lee, S.-W.; Suen, C.Y. Thinning methodologies-a comprehensive survey. *IEEE Trans. Pattern Anal. Mach. Intell.* **1992**, *14*, 869–885. [CrossRef]
8. Rosenfeld, A.; Pfaltz, J.L. Sequential Operations in Digital Picture Processing. *J. ACM* **1966**, *13*, 471–494. [CrossRef]
9. Rosenfeld, A.; Pfaltz, J.L. Distance functions on digital pictures. *Pattern Recognit.* **1968**, *1*, 33–61. [CrossRef]
10. Borgefors, G. Distance transformations in digital images. *Comput. Vis. Graph. Image Process.* **1986**, *34*, 344–371. [CrossRef]
11. Akmal Butt, M.; Maragos, P. Optimum design of chamfer distance transforms. *IEEE Trans. Image Process.* **1998**, *7*, 1477–1484. [CrossRef]
12. Danielsson, P.-E. Euclidean distance mapping. *Comput. Vis. Graph. Image Process.* **1980**, *14*, 227–248. [CrossRef]
13. Ye, Q.-Z. The signed Euclidean distance transform and its applications. In Proceedings of the 9th International Conference on Pattern Recognition, Rome, Italy, 14 May–17 November 1988; IEEE Computer Society Press: Rome, Italy, 1988; pp. 495–499.
14. Leymarie, F.; Levine, M.D. Fast raster scan distance propagation on the discrete rectangular lattice. *CVGIP Image Underst.* **1992**, *55*, 84–94. [CrossRef]
15. Ragnemalm, I. The Euclidean distance transform in arbitrary dimensions. *Pattern Recognit. Lett.* **1993**, *14*, 883–888. [CrossRef]
16. Cuisenaire, O.; Macq, V. Fast and exact signed Euclidean distance transformation with linear complexity. In Proceedings of the ICASSP99 (Cat. No.99CH36258), Phoenix, AZ, USA, 15–19 March 1999; Volume 6, pp. 3293–3296.
17. Shih, F.Y.; Wu, Y.-T. The Efficient Algorithms for Achieving Euclidean Distance Transformation. *IEEE Trans. Image Process.* **2004**, *13*, 1078–1091. [CrossRef] [PubMed]
18. Shih, F.Y.; Wu, Y.-T. Fast Euclidean distance transformation in two scans using a 3 × 3 neighborhood. *Comput. Vis. Image Underst.* **2004**, *93*, 195–205. [CrossRef]

19. Grevera, G.J. The "dead reckoning" signed distance transform. *Comput. Vis. Image Underst.* **2004**, *95*, 317–333. [CrossRef]
20. Paglieroni, D.W. Distance transforms: Properties and machine vision applications. *CVGIP Graph. Models Image Process.* **1992**, *54*, 56–74. [CrossRef]
21. Paglieroni, D.W. A unified distance transform algorithm and architecture. *Mach. Vis. Appl.* **1992**, *5*, 47–55. [CrossRef]
22. Saito, T.; Toriwaki, J.-I. New algorithms for euclidean distance transformation of an n-dimensional digitized picture with applications. *Pattern Recognit.* **1994**, *27*, 1551–1565. [CrossRef]
23. Piper, J.; Granum, E. Computing distance transformations in convex and non-convex domains. *Pattern Recognit.* **1987**, *20*, 599–615. [CrossRef]
24. Verwer, B.J.H.; Verbeek, P.W.; Dekker, S.T. An efficient uniform cost algorithm applied to distance transforms. *IEEE Trans. Pattern Anal. Mach. Intell.* **1989**, *11*, 425–429. [CrossRef]
25. Ragnemalm, I. Neighborhoods for distance transformations using ordered propagation. *CVGIP Image Underst.* **1992**, *56*, 399–409. [CrossRef]
26. Eggers, H. Two Fast Euclidean Distance Transformations in Z2 Based on Sufficient Propagation. *Comput. Vis. Image Underst.* **1998**, *69*, 106–116. [CrossRef]
27. Sharaiha, Y.M.; Christofides, N. A graph-theoretic approach to distance transformations. *Pattern Recognit. Lett.* **1994**, *15*, 1035–1041. [CrossRef]
28. Falcao, A.X.; Stolfi, J.; de Alencar Lotufo, R. The image foresting transform: Theory, algorithms, and applications. *IEEE Trans. Pattern Anal. Mach. Intell.* **2004**, *26*, 19–29. [CrossRef] [PubMed]
29. Cuisenaire, O.; Macq, B. Fast Euclidean Distance Transformation by Propagation Using Multiple Neighborhoods. *Comput. Vis. Image Underst.* **1999**, *76*, 163–172. [CrossRef]
30. Cao, T.-T.; Tang, K.; Mohamed, A.; Tan, T.-S. Parallel Banding Algorithm to compute exact distance transform with the GPU. In Proceedings of the ACM SIGGRAPH Symposium on Interactive 3D Graphics and Games-I3D 10, Maryland, MD, USA, 19–21 February 2010; ACM Press: Washington, DC, USA, 2010; p. 83.
31. Manduhu, M.; Jones, M.W. A Work Efficient Parallel Algorithm for Exact Euclidean Distance Transform. *IEEE Trans. Image Process.* **2019**, *28*, 5322–5335. [CrossRef]
32. de Assis Zampirolli, F.; Filipe, L. A Fast CUDA-Based Implementation for the Euclidean Distance Transform. In Proceedings of the 2017 International Conference on High Performance Computing & Simulation (HPCS), Genoa, Italy, 17 July 2017; IEEE: Genoa, Italy, 2017; pp. 815–818.
33. Rong, G.; Tan, T.-S. Jump flooding in GPU with applications to Voronoi diagram and distance transform. In Proceedings of the 2006 symposium on Interactive 3D graphics and games-SI3D '06, Redwood City, CA, USA, 14–17 March 2006; ACM Press: Redwood City, CA, USA; p. 109.
34. Zheng, L.; Gui, Z.; Cai, R.; Fei, Y.; Zhang, G.; Xu, B. GPU-based efficient computation of power diagram. *Comput. Graph.* **2019**, *80*, 29–36. [CrossRef]
35. Schneider, J.; Kraus, M.; Westermann, R. GPU-based real-time discrete Euclidean distance transforms with precise error bounds. In Proceedings of the Fourth International Conference on Computer Vision Theory and Applications, Lisboa, Portugal, 5 February 2009; SciTePress—Science and Technology Publications: Lisboa, Portugal, 2009; pp. 435–442.
36. Honda, T.; Yamamoto, S.; Honda, H.; Nakano, K.; Ito, Y. Simple and Fast Parallel Algorithms for the Voronoi Map and the Euclidean Distance Map, with GPU Implementations. In Proceedings of the 2017 46th International Conference on Parallel Processing (ICPP), Bristol, UK, 14 August 2017; IEEE: Bristol, UK, 2017; pp. 362–371.
37. Cao, T.-T.; Tang, K.; Mohamed, A.; Tan, T.-S. Parallel Banding Algorithm Plus to Compute Exact Distance Transform with the GPU. Available online: https://www.comp.nus.edu.sg/~{}tants/pba.htm (accessed on 22 September 2020).